Received: 8 January 2021 | Revised: 3 January 2022 | Accepted: 11 July 2022

DOI: 10.1002/stc.3052

RESEARCH ARTICLE

WILEY

Modal identification of storage racks for cheese wheels

Claudio Bernuzzi[1] | **Carlo Rottenbacher**[2] | **Marco Simoncelli**[1] | **Paolo Venini**[3]

[1]Department of Architecture, Built Environment and Construction Engineering, Politecnico di Milano, Milan, Italy

[2]Department of Electrical, Computer and Biomedical Engineering, Università degli Studi di Pavia, Pavia, Italy

[3]Department of Civil Engineering and Architecture, Università degli Studi di Pavia, Pavia, Italy

Correspondence
Marco Simoncelli, Department of Architecture, Built Environment and Construction Engineering, Politecnico di Milano, Milan, Italy.
Email: marco.simoncelli@polimi.it

Summary

During the Emilia-Romagna earthquake (2012), a great number of steel racks used to store cheese wheels collapsed, causing a non-negligible damage to the Italian economy. Therefore, for similar structures that survived and are in service, a deep investigation towards the assessment of their effective safety is required.

In the seismic analysis of these frames, the mechanical constraint acting onto the racks due to the reinforced concrete sidewalls, possible nonlinearities exhibited by the base-plate joints and the in-plane restraint provided by wooden boards that connects adjacent columns should be carefully modelled to ensure realistic design results.

In the paper, an experimental activity, based on suitable modal identification techniques, is presented to capture the dynamic behaviour of these peculiar structures. The scope is to collect data useful to calibrate numerical finite element models in order to accurately define the aforementioned unknown parameters. Furthermore, a few numerical models based on ideal restraints are herein discussed stressing out non-negligible differences in terms of expected seismic and static response.

KEYWORDS

FE analysis, modal identification, seismic performance, steel rack for cheese wheels, vibrations

1 | INTRODUCTION

Earthquakes occurred in May 2012 in Emilia-Romagna (Italy) caused severe damages to industrial reinforced concrete buildings[1] and to the contained steel framed systems typically employed to store goods and products, that is, the so-called storage racks. Racks used to store cheese wheels, identified in the following as cheese racks, represent the typology of racks that underwent the most severe damage. In the past, cheese racks were composed by hot-rolled welded components, while, starting from a few years ago, a new typology of frames made by cold-formed steel members[2] showed up, which resemble traditional storage pallet racks[3] and are nowadays extensively employed. This manuscript is focused on the former type of racks (Figure 1a) that are composed by a set of battened steel columns (Figure 1b). Composite action is in the transversal (cross-aisle) direction: chords are two tubular profiles connected through their full height (in general, in the range 4–8 m). Base tubes are welded to a horizontal I-shaped beam, simply supported on an industrial concrete floor without any kind of mechanical anchor system (Figure 1c). Battens are horizontal L-profiles

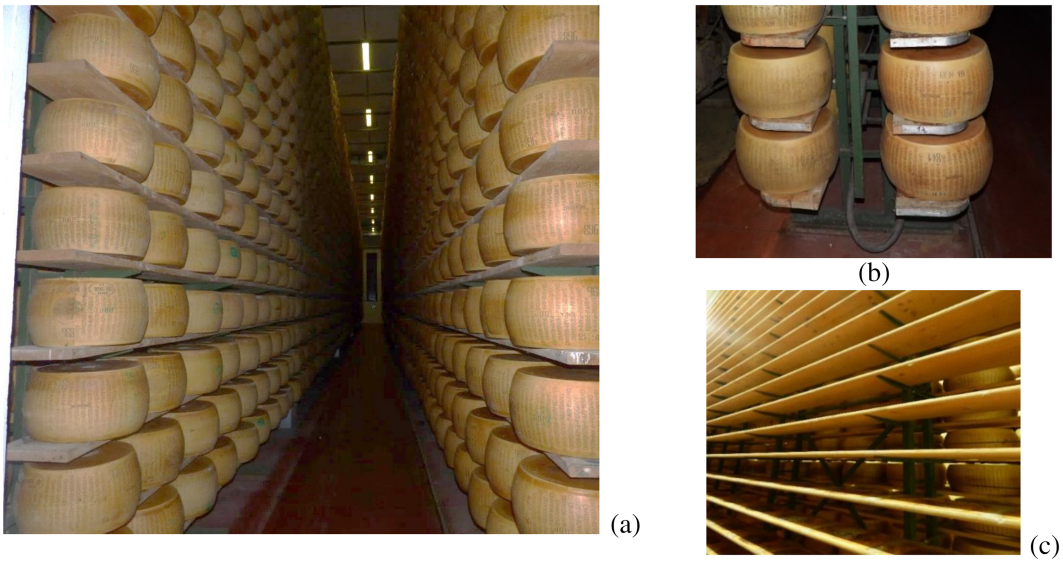

FIGURE 1 Typical cheese racks: (a) global view and (b) detail of the column-bases and (c) of wooden boards supporting cheese wheels

FIGURE 2 Typical collapse of cheese racks after by the Emilia Romagna seismic sequence (2012)

(angles) vertically spaced at 330 mm and protruded beyond the steel columns as cantilever beams supporting the wood boards, on which cheese wheels are directly located. In the longitudinal (down-aisle) direction, the built-up columns are connected to each other by wooden boards equally spaced at 1.5 m, allowing to store three wheels in each bay per side. Longitudinal X-type bracings are characterised by components welded to the angles by means of fillets having a limited throat. The typical cheese rack system is composed by a set of frames realised by composite columns connected with the wood boards, separated by aisles (Figure 1a), that allows picking, cleaning and brushing of the cheese wheels during the ageing period (12–40 months).

Cheese racks of the oldest type have been erected since the beginning of the last century relying on the blacksmith expertise, that is, with very poor structural checks and neglecting all the aspects associated with safety against earthquakes. For this reason, during the 2012 earthquakes, they collapsed unexpectedly causing a *domino* effect (progressive collapse) leading, as previously mentioned, to relevant damages to the many thousands of tons of cheese stored in each of the several damaged warehouses (Figure 2).

Static and seismic design of adjustable storage racks has been deeply studied in literature[4–8] but quite limited attention has been paid to cheese racks that behave[9] in a significantly different way from the traditional storage racks. Adjustable steel storage pallet racks are characterised by a skeleton frame that is unbraced in the longitudinal direction (like the classic steel moment resisting frames for buildings) and braced in the transversal one and can dissipate seismic

energy throughout their beam-to-column and base-plate connections. Concerning the seismic behaviour, in addition to the expected structural damages earthquake accelerations frequently cause also the falling or toppling of the stored goods,[10,11] which can bring to the overall collapse of the system. As to cheese racks, the structural scheme is remarkably different, as discussed in Section 2 and, during the earthquakes, the collapse is mainly due to the low redundancy of the resisting system and to the effect associated with the sliding of cheese wheels. Despite it is well-known that an important reduction of seismic vulnerability of storage racks can be obtained by using efficient base-isolation as well as passive control techniques,[12,13] no evidence is up-to-now available on the direct applicability of the associated research outcomes to cheese rack typologies.

A research project is currently in progress in collaboration between the Politecnico di Milano and the Università di Pavia on the design rules for cheese racks. In the present paper, attention is addressed to cheese racks of the old type: an experimental activity, based on the modal identification techniques, is performed on two frame typologies differing for the number of bays and load levels. The aim of the in-situ tests is to capture the rack dynamic behaviour needed for calibration of the actual degrees of restraint provided by column bases, wood boards and connections to the warehouse. It is worth mentioning that an accurate evaluation of these data is a fundamental pre-requisite for the following:

- safety evaluation of existing structures under earthquakes;
- defining suitable strengthening techniques.

2 | THE GEOMETRY OF THE CONSIDERED CHEESE RACKS

Two types of cheese racks have been considered, which are herein identified as CR1 and CR2 type; they mainly differ from each other by the number of load levels and of horizontal restraints to the lateral reinforced concrete walls of the warehouse. In both frames, battened built-up columns (Figure 3a) are composed in the cross-aisle direction by two vertical tubular profiles (50 × 50 mm with a thickness of 4 mm) welded through their full height to L profile (20 × 40 × 4 mm for type CR1 and 25 × 40 × 4 mm for type CR2), as showed in Figure 3b. At the base, the tubes are welded to an INP100 I-shaped beam, simply resting on the floor without anchors (Figure 3c). On the column top, tubular members connect the cheese racks to each other in the cross-aisle direction (Figure 4a), while in the down-aisle the

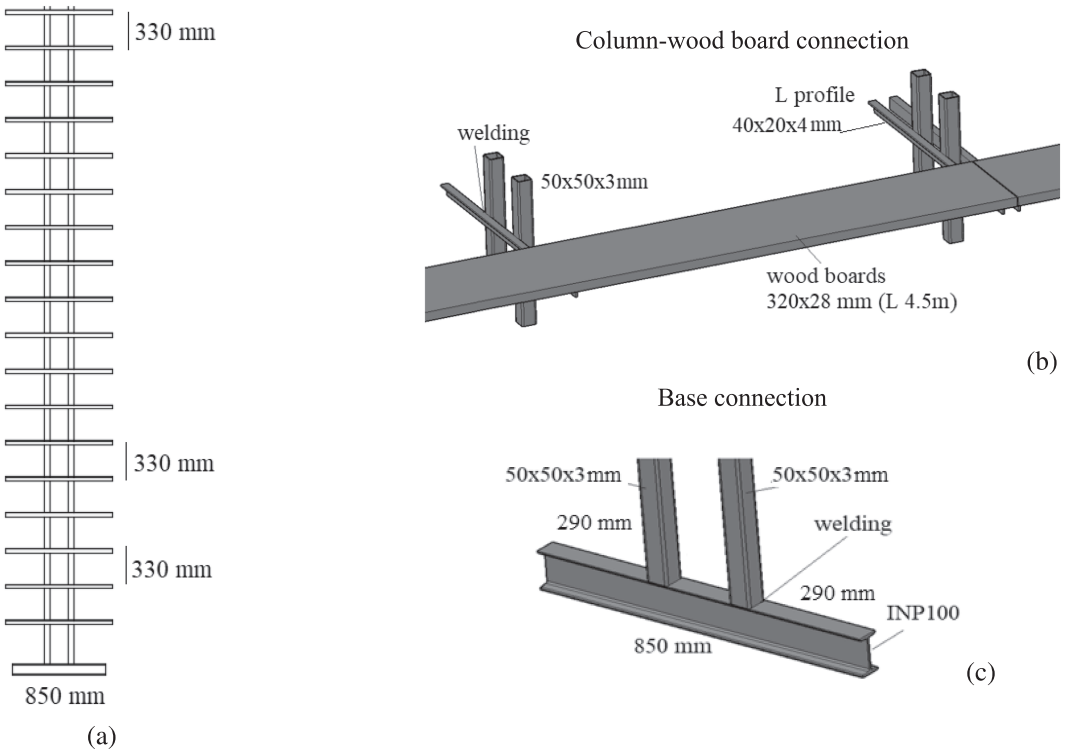

FIGURE 3 Typical components and dimensions in storage racks for cheese wheels

FIGURE 4 Typical racks to wall connection: (a) top connections, (b, c) view of the cantilever beams, (d) vertical elements and (e) wall connections

FIGURE 5 Typical vertical bracing systems for (a) type CR1 and (b) CR2 type

external composite columns are linked via tubes (Figure 4e) to the reinforced concrete building walls. A complete view of cantilever beams connected to the wooden boards is proposed in Figure 4b,c together with the view of the battened columns (Figure 4d).

Longitudinal X-bracings, able to resist only to tension forces, are located in the external bays. The column bases, unlike in the more traditional carpentry frames, are not directly connected to the diagonals: in the first panel they are located 600 mm above the ground level. This discontinuity on the bracing systems brings the forces into the column instead on the ground and affects the seismic response of the whole system. In CR1, the horizontal elements that should complete the truss bracing are missing (Figure 5a) unlike in CR2 (Figure 5b) rack type.

In Figure 6, all the details of both models for the FE analyses are reported. Structural steel members (tubes, angles, links and diagonals) are modelled via *beam* elements, like the wood boards that have been considered continuous within the whole length of the racks.

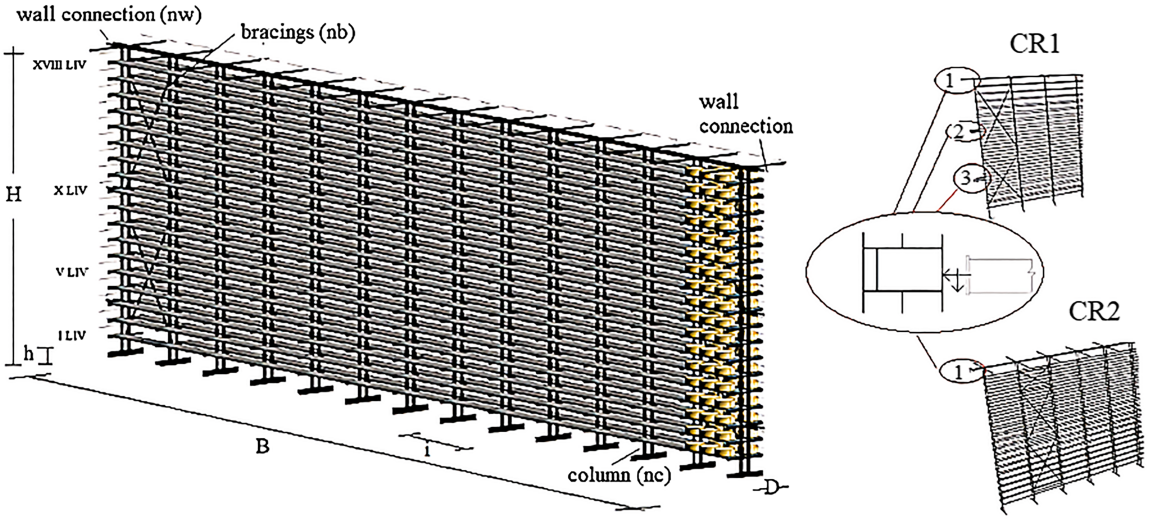

	Depth (D)	Spacing (l)	Total length (H)	Total height (H)	Interstorey height (h)	number of columns (ne)	number of storage levels (ns)	number of bracing towers (nb)	number of link-to-wall connections (nw)	average weight of wheel (W)
CR1	850mm	1500mm	21000mm	6750mm	330mm	14	18	2	3+3	41.5 kg
CR2	850mm	1500mm	42000mm	7500mm	330mm	28	20	3	1+1	40.8 kg

FIGURE 6 Peculiarities of the two considered rack cheese models

3 | UNCERTAINTIES RELATED TO OVERALL BEHAVIOUR

Seismic behaviour of cheese racks is quite complex to predict because directly influenced by parameters subject to uncertainties that include the following:

1. Base-plate connections (Figure 1c). In routine design, base-plate connections are modelled via the alternative ideal restraints of hinges or fixed bases, neglecting hence their action, strictly depending on the level of the axial force, as recently demonstrated by researchers on the more traditional steel storage pallet racks[14].
2. Lateral connections with the vertical walls of the warehouse (Figure 4c). These restraints should be simulated via external axial springs, whose stiffness accounts for the effective performance of both steel members and concrete walls. Also in this case, ideal restraints are usually considered in routine design.
3. Continuity provided by the wood boards. Despite the expected influence on the overall behaviour, these components are generally considered as non-structural elements and hence the data related to their effective stiffness are totally ignored in routine design.

3.1 | Evaluation of frequencies of vibration and buckling load

To demonstrate how these parameters can influence remarkably the overall response, a preliminary numerical analysis has been carried out by considering the cases described in Table 1. Self-weight of wood boards and structural steel elements has been evaluated by assuming the material density equal to 4.5 and 78.6 kN/m^3, respectively. Cheese wheels have been modelled as uniform distributed loads along the wood boards. Owing to the absence of data about the effective degree of the restraint, perfectly fixed or pinned bases have been assumed. Moreover, concerning the lateral restraints along the down-aisle direction, the two extreme cases have been considered, that is, the presence or the absence of lateral supports preventing the horizontal rack displacements, identified in Table 1 with Prevented or Free case, respectively. Wood boards, whose continuity between columns influences longitudinal buckling modes, are currently neglected in the structural analysis model used in routine practice. They have been herein modelled as continuous *beam* elements with an Elastic modulus (E_w) of 100 or 16,000 MPa. Assuming for E_w an even lower value than 100 MPa would lead to undesired incompatible buckling modes whereas 16,000 MPa is the value recommended by standard codes for spruce wood material.

TABLE 1 Considered parameters on the different models

Model	Base	Lateral displacement at the anchors	E_w [MPa]
CR1_A	Pinned	Free	100
CR1_B	Fixed	Free	16,000
CR1_C	Fixed	Prevented	16,000
CR1_D	Fixed	Prevented	100
CR1_E	Pinned	Prevented	16,000
CR2_A	Pinned	Free	100
CR2_B	Fixed	Free	16,000
CR2_C	Fixed	Prevented	16,000
CR2_D	Fixed	Prevented	100
CR2_E	Pinned	Prevented	16,000

TABLE 2 Buckling and key modal analyses results

		Frequencies (% modal mass and deformed shape direction)			
Model	Buckling α_{cr}	I mode	II mode	III mode	IV mode
CR1_A	2.51	0.711 Hz (86% down)	1.890 Hz (70% cross)	1.950 Hz (15% cross)	3.650 Hz (15% down)
CR1_B	5.67	0.745 Hz (83% down)	1.950 Hz (75% cross)	3.155 Hz (7% down)	3.688 Hz (15% cross)
CR1_C	14.65	2.091 Hz (75% cross)	3.372 Hz (77% down)	4.137 Hz (10% cross)	5.636 Hz (15% down)
CR1_D	13.84	1.894 Hz (75% cross)	2.273 Hz (88% down)	2.950 Hz (15% cross)	4.216 Hz (15% down)
CR1_E	9.56	1.991 Hz (75% cross)	3.172 Hz (10% cross)	3.737 Hz (55% down)	4.026 Hz (28% down)
CR2_A	2.25	0.475 Hz (85% down)	1.429 Hz (75% cross)	1.662 Hz (2% down)	1.778 Hz (10% cross)
CR2_B	5.17	0.982 Hz (80% down)	1.634 Hz (74% cross)	1.750 Hz (6% down)	1.887 Hz (11% cross)
CR2_C	5.18	1.078 Hz (75% down)	1.629 Hz (74% cross)	1.850 Hz (11% down)	2.341 Hz (5% cross)
CR2_D	4.93	0.799 Hz (75% down)	1.329 Hz (75% cross)	1.551 Hz (12% down)	2.551 Hz (15% cross)
CR2_E	2.47	0.788 Hz (81% down)	1.559 (74% cross)	1.645 Hz (11% down)	3.548 Hz (5% cross)

Starting from the original models, five different combinations of the previously mentioned parameters have been considered for each cheese rack (labelled in the following _A, _B, _C, _D and _E) generating in total 10 different FE models, whose key features are summarised in Table 1.

Numerical analyses have been carried out to evaluate the elastic buckling multipliers (α_{cr}) and the key parameters governing seismic design.[15,16] In Table 2, the values of α_{cr} are reported together with the first three frequencies of vibration with significative % of participation mass (i.e., >5%). Local modes of the wooden boards are not considered. The percentage of the participant mass and the main direction of the deformed shape are specified between brackets.

Though the number of cases considered hereafter is rather limited, it suffices to assess the influence of the different design assumptions on the effective rack behaviour. In particular, it can be noted that

- the influence of the wood board properties can be directly evaluated by comparing the results associated with the _C and _D models. By considering $E_w = 16{,}000$ MPa instead of 100 MPa, the term α_{cr} increases moderately (6% and 5% for CR1 and CR2 type, respectively) and the fundamental frequency of vibration reduces of 10% for CR1 and 34% for CR2. The variation of the percentage of the participation masses is negligible;
- the influence of the column bases is always non-negligible, as it appears directly from data related to the _C and _E models. By considering a pinned base (_E) instead of a fixed one (_C), the buckling load multiplier decreases (53% and up to 2 times for CR1 and CR2, respectively). Moreover, the predominant frequency decreases moderately (5%) for CR1, characterised by a deformation in cross-aisle direction, and more remarkably (36%) for CR2, where instead the deformation is in the down-aisle direction;

- the influence of the links to the concrete walls of the warehouse can be appraised by considering the _B and _C cases. In CR1, 3 links are located on each external column. Their presence influence significantly the overall response increasing both the critical load multiplier (2.6 times) and the fundamental frequency (2.8 times) and modifying the direction of the modal deformed shape, as highlighted in Figure 7. In particular, in case of no links (Figure 7a) the deformed modal shape is in the down-aisle plane; when the rack is connected to the shear walls (Figure 7b) the first modal shape became predominant in the cross-aisle direction. On the contrary, if CR2 is observed, it can be concluded that the presence of only one connection influences moderately the overall behaviour, as it appears by comparing α_{cr} and the frequencies for CR2_B and CR2_C (Figure 8). The link, if present, is located on the top of the external column and hence is not effective to reduce the effective length of the columns, mainly influenced by the height of the vertical bracing panels, unlike in CR1. It can be appraised also by considering the buckling deformed shapes and the critical buckling load (N_{cr}), which are depicted in Figure 8. Similarities can be, in fact, observed for CR2_B and CR2_C models, confirming the modest effect of only a top link. Furthermore, in the figure, the change of curvature in the buckling shape has been highlighted with a red arrow.

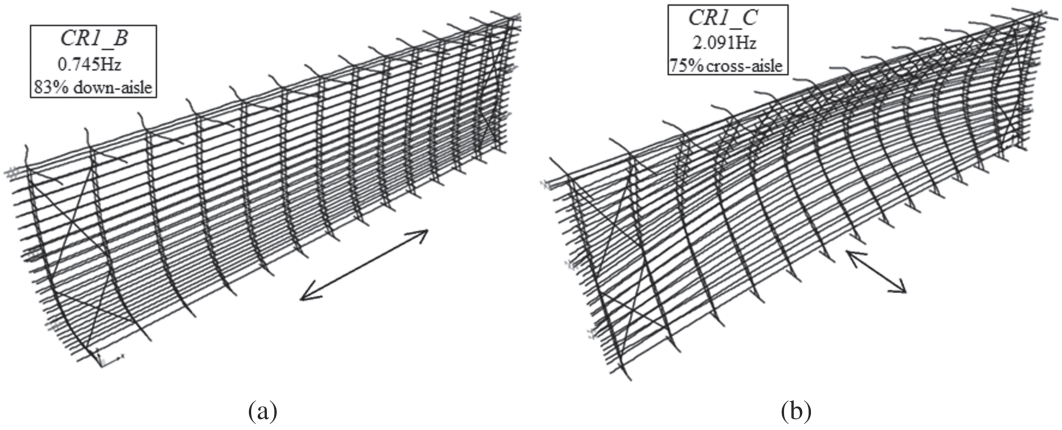

FIGURE 7 Deformed modal shape associated with the first mode for (a) CR1_B with no links and (b) CR1_C with three links

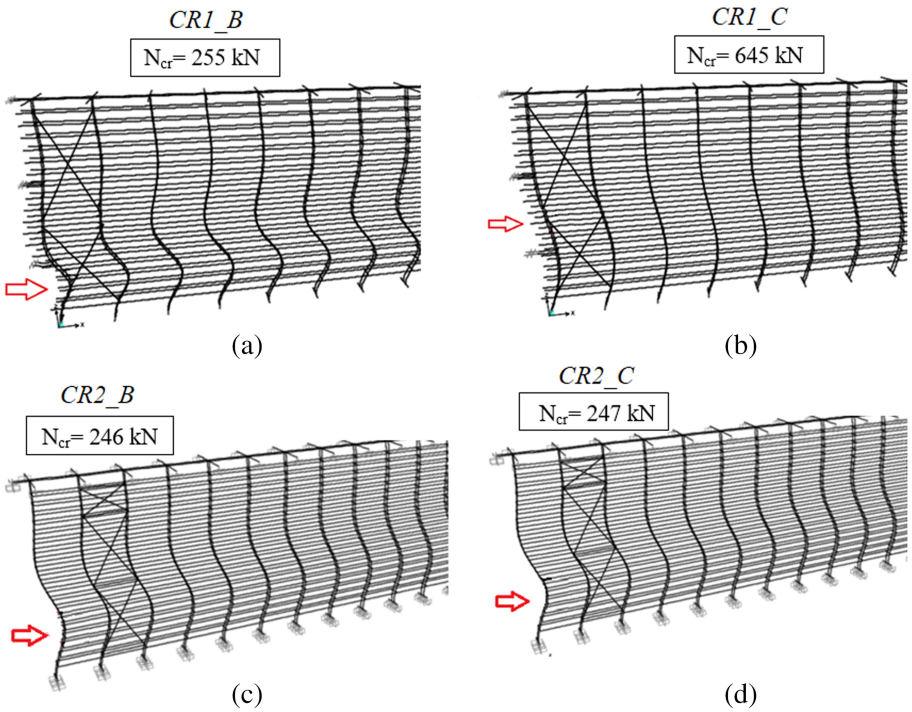

FIGURE 8 Buckling deformed shape of (a) CR1_B, (b) CR1_C, (c) CR2_B and (d) CR2_C models

The great differences previously discussed on the five different models developed for the two rack typologies underline the need of a refined calibration of the three considered parameters. The associated differences in terms of buckling multiplier and frequencies produce inevitably second order effects on the frames and, consequently, different overall responses under the same set of earthquakes to be considered in the seismic design. For this reason, an experimental modal identification procedure,[17,18] which is described in the following, is always necessary and strongly required before the design analysis.

3.2 | Evaluation of static and seismic performance

The results obtained in paragraph Section 3.1 underline the importance of the structural uncertainties on the overall response of cheese racks. In particular, the critical load multiplier and the frequencies of vibration were discussed, which affect directly also the safety of the considered structures. Referring to the General Method (GEM) of the Eurocode 3-1-1,[19] the safety index (SI) of the most stressed element could be suitably defined as

$$SI_i^{GEM} = \frac{\gamma_M}{\chi_{op}\alpha_{ult,k,i}} \leq 1.0 \tag{1}$$

where χ_{op} is the stability reduction factor related to the relative slenderness, λ_{op}:

$$\lambda_{op} = \sqrt{\frac{\alpha_{ult,k,i}}{\alpha_{cr,i}}} \tag{2}$$

$\alpha_{ult,k,i}$ is the minimum load amplifier of the design loads to reach the characteristic resistance in the most stressed cross-section, defined as

$$\alpha_{ult,k,i} = \frac{1}{SI_i^R}; \tag{3a}$$

$$SI_i^R = \frac{N_{Ed,i}}{N_{Rd}} + \frac{M_{y,Ed.i}}{M_{y,Rd}} + \frac{M_{z,Ed,i}}{M_{z,Rd}} \tag{3b}$$

where $N_{Ed,i}$, $M_{y,Ed,i}$ and $M_{z,Ed,i}$ are the acting axial force and bending moments of the considered load combination, while N_{Rd}, $M_{y,Rd}$ and $M_{z,Rd}$ are the resistance values, which depend on the cross-sections characteristics and on the yielding tension. Subscript i is related to the considered load combination, since the internal forces could derive from static or seismic analyses, which lead to SI_{ULS}^{GEM} or SI_{SLV}^{GEM}, respectively. According to the Italian standard at the ultimate limit state (ULS), the live loads (i.e., cheese wheels) have to be amplified by a factor of 1.5, while a factor 1.3 amplifies the self-weight. No amplification factors are conversely applied when defining seismic load combinations (SLV). The columns of the considered racks are class 1 profiles, according to the classification criteria of EN1993-1-1[19] and the material is steel S235.

For the seismic evaluation, the Modal Response Spectrum Analysis (MRSA) has been performed considering a spectrum located in the centre of Italy (Emilia-Romagna) with a peak ground acceleration equal to $a_g = 0.09\ g$. Finally, the behaviour factor *(q)* was assumed equal to 1.5. All the analyses take into account the second order effects, independently of the value of the buckling multipliers of Table 2. By applying the previous equations to the considered structural analyses, the obtained SI are presented in Table 3. The SI_{SLV}^{GEM} is the maximum between all the seismic combinations required by the Italian building code.

The buckling factors of Table 2 were obtained without amplification factors on the applied loads, as in the seismic combination, therefore at ULS their value decrease of a factor equal to about 1.5 ($\alpha_{cr,SLV} \approx 1.5\alpha_{cr,ULS}$). If the static load condition is considered, both frames are always on the safe side independently of the choice of the structural parameters. However, considering the maximum and the minimum of each group, a great dispersion of the values can be observed: 40% and 35% of differences for CR1 and CR2, respectively. The worst cases for the static design are the _A for both racks, that is, the one with the lowest buckling factor. For the seismic combinations the worst cases became the

TABLE 3 SI estimation of the considered frames

Model	CR1_A	CR1_B	CR1_C	CR1_D	CR1_E	CR2_A	CR2_B	CR2_C	CR2_D	CR2_E
SI_{SLU}^{GEM}	0.66	0.51	0.43	0.42	0.47	0.74	0.51	0.51	0.53	0.72
SI_{SLV}^{GEM}	0.48	1.22[a]	1.34[a]	1.27[a]	1.18[a]	0.55	0.90	0.96	0.92	0.89

[a]Not verified.

_C ones for both racks. Moreover, the presence of fixed bases generates bending moments on the bottom in both longitudinal and transversal directions. Comparing the maximum with the minimum also for this combinations, differences up to 2.8 times can be observed. Results remark once again the importance of a good calibration of the structural parameters prior to the structural analyses.

Finally, as an example of the SI distribution, in case of both seismic and static load combinations, Figure 9 can be considered for CR1_C frame. In particular, the maximum SI on all the columns is plotted together with the details of the SI distribution along the height for a selected internal and external column.

4 | THE EXPERIMENTAL PROGRAMME

An experimental campaign was carried out with the aim to identify the modal behaviour, that is, eigenvalues and associated modal shapes, of the considered CR1 and CR2 racks.

4.1 | Tests description

Experimental tests were performed in both the down- and cross-aisle direction. Test set-up (Figure 10a) was comprised of three PCB-393A03 mono-axial piezoelectric accelerometers[20] (Figure 10c,d) with a sensitivity of 1000 mmV/g connected to IEPE National Instrument board with three channels.[21] A constant excitation energy is given to the structure via an on-purpose built impact hammer, kinematically similar to a Charpy test machine (Figure 10b). The impact hammer was rigidly connected at the top of the rack to one of the two tubes of the built-up column. The height of falling (250 mm) and the excitation mass (300 *g*) generate a constant input energy during each test, which is an essential prerequisite to guarantee the reliability of the results. The combination of the weight and mass was skilfully chosen to generate an impact force adequate to excite the frequency range of interest. The accelerations were recorded with a sampling frequency of 6400 Hz ($\Delta t = 0.156$ ms). Given the limited number of available transducers that is not sufficient to obtain directly the desired spatial resolution for the mode shape estimates, an adequate number of tests has been executed implementing a strict test protocol.

According to the adopted experimental protocol, an accelerometer served as reference sensor and was therefore given a fixed position whereas the remaining two transducers were cleverly moved from test to test along the height of the structures and/or from bay to bay, until the structural response is measured at all the pre-defined desired locations in order to cover all the points of interest. Tables 4 and 5 report the schemes adopted for the multiple locations of the accelerometers, which are related to tests in the longitudinal and transversal direction, respectively. If both tables are considered, label *Ci* is related to the number of *i*th column while label S_i indicates the *i*th storage level.

It is worth to highlight that the position of each accelerometer was decided according to a preliminary modal analysis executed on the FEM models discussed in Section 3. Moreover, to better clarify the experimental protocol, one test configuration in down-aisle directions is sketched in Figure 11. In the same figure, label F indicates the input force whereas the transducers channels were indicated with their progressive number (0, 1 and 2) and the associated global direction (*X*).

After the positioning of all the transducers for the specific test, the impact hammer was released three times consecutively with an intermediate stop of about 3 s, recording three different accelerations on each transducer. In Figure 12, an example of the recorded time-history (acceleration, *a*, in *g* versus time, *t*, in seconds) from the channel 0 of the CR1_CROSS_Y_T2 configuration is reported together with the associated fast Fourier transform (FFT) developed according to the procedure deeply discussed in Duhamel and Vetterli.[22] The peaks in this graphical view indicate the

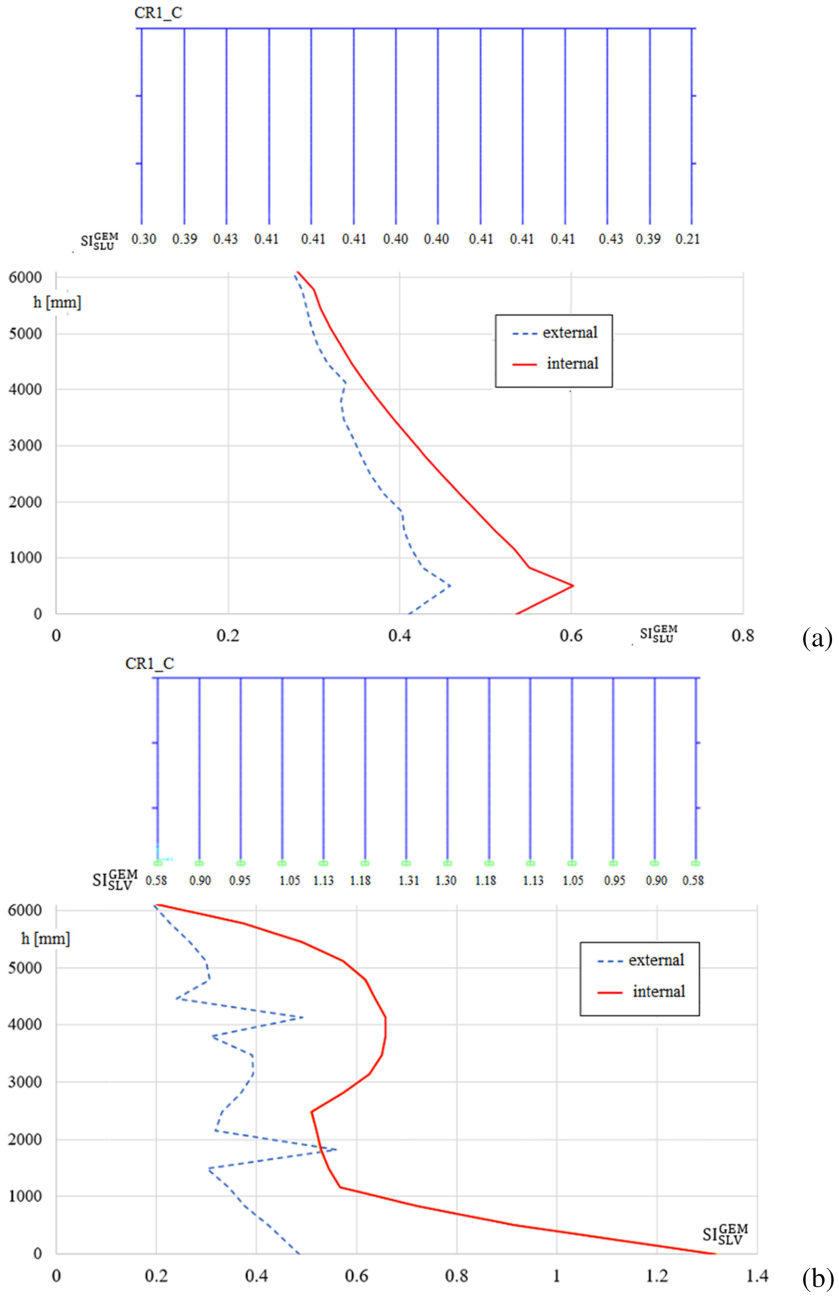

FIGURE 9 Complete checks of CR1_C frame: (a) ultimate limit state and (b) seismic load combination

presence of predominant frequencies in the signal. It can be observed a big difference in term of Energy (Magnitude) between peaks and the frequencies around them, meaning that no issues regarding noise can be detected.

4.2 | Re-elaboration of the test data

The modal parameters estimated by applying the well-known Frequency Domain Decomposition (FDD) technique[23] are herein presented and discussed. This method is based on the evaluation of the spectral matrix (i.e., the matrix of cross-spectral densities) in the frequency domain. After the evaluation of the spectral matrix, the Singular Value Decomposition (SVD) at each frequency has been developed. The inspection of the SVD graphs permits to identify the resonant frequencies and arrive at an estimate the corresponding mode shape. This technique allows a rather

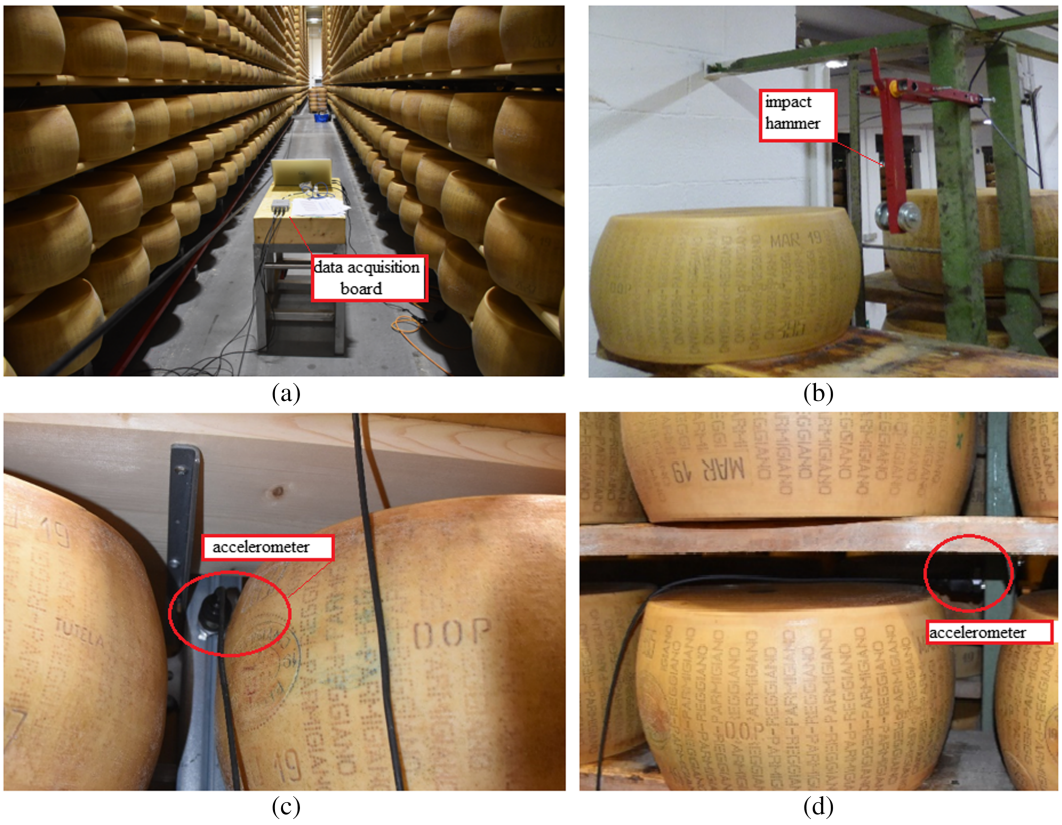

FIGURE 10 View of (a) test set-up and acquisition board, (b) impact hammer device and (c, d) accelerometer location

TABLE 4 Location of accelerometers, down_X direction

CR1	ch	T1	T2	T3	T4	T5	T6	T7	T8	T9	T10
	0	C2,S3	C2,S3	C2,S3	C2,S3	C2,S3	C2,S3	C13,S3	C13,S3	C13,S3	C13,S3
	1	C2,S6	C2,S10	C2,S15	C4,S6	C6,S6	C8,S6	C8,S6	C8,S18	C10,S6	C13,S6
	2	C2,S8	C2,S12	C2,S8	C4,S8	C6,S8	C8,S8	C8,S8	C8,S16	C10,S8	C13,S8
CR2	ch	T1	T2	T3	T4	T5	T6	T7	T8	T9	T10
	0	C2,S4	C2,S4	C2,S4	C2,S4	C2,S4	C2,S4	C2,S4	C2,S4	C28,S4	C28,S4
	1	C2,S6	C2,S12	C2,S18	C4,S6	C6,S6	C8,S6	C10,S6	C12,S6	C28,S6	C26,S6
	2	C2,S9	C2,S14	C2,S20	C4,S9	C6,S9	C8,S9	C10,S9	C12,S9	C28,S9	C26,S9

TABLE 5 Location of accelerometers, cross_Y direction

CR1	ch	T1	T2	T3	T4	T5	T6
	0	C2,S4	C2,S4	C4,S4	C6,S4	C8,S4	C11,S4
	1	C2,S6	C2,S6	C4,S6	C6,S6	C8,S6	C11,S6
	2	C2,S9	C2,S9	C4,S9	C6,S9	C8,S9	C11,S9
CR2	ch	T1	T2	T3	T4	T5	T6
	0	C14,S4	C14,S4	C14,S4	C21,S4	C24,S4	C28,S4
	1	C14,S6	C16,S6	C18,S6	C21,S6	C24,S6	C28,S6
	2	C14,S9	C16,S9	C18,S9	C21,S9	C24,S9	C28,S9

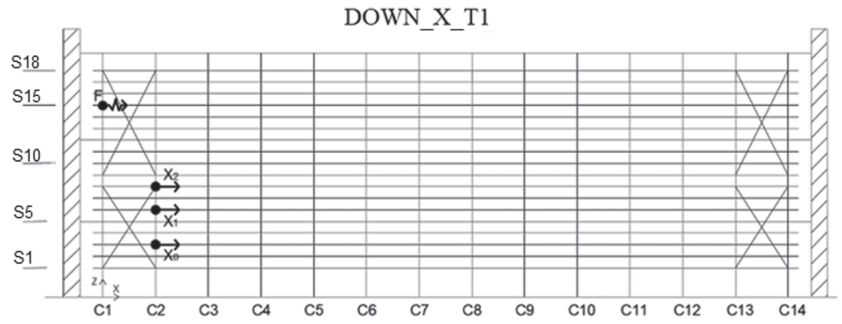

FIGURE 11 Example of test set-up in down-aisle (*X*) direction for CR1

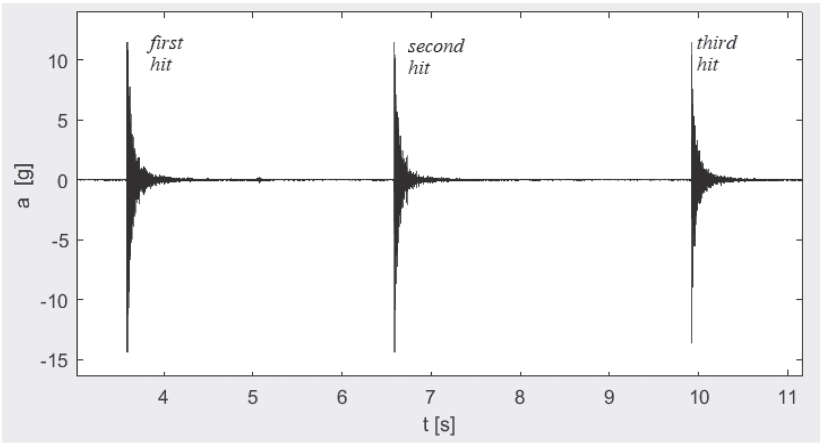

(a)

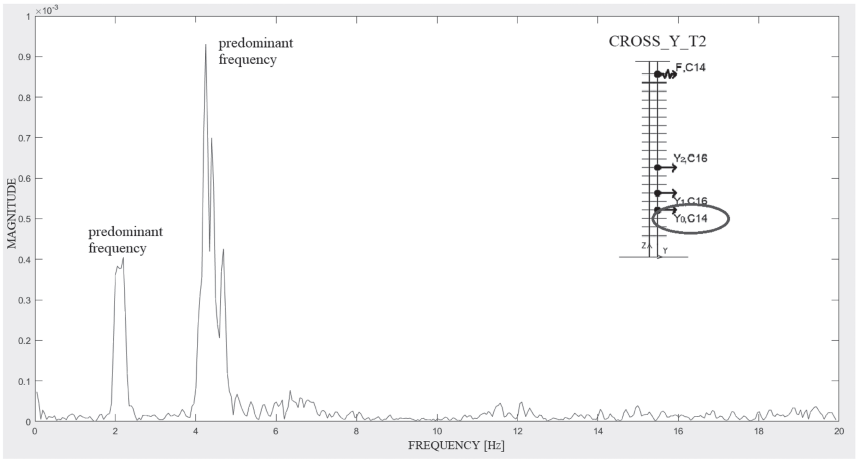

(b)

FIGURE 12 Results obtained from channel 0 in test CR1_CROSS_Y_T2: (a) acceleration time-history and (b) the associated fast Fourier transform (FFT)

straightforward separation of the predominant structural frequencies from noise. In Figures 13 and 14 first singular value of the spectral matrix with all the elaborated signals are presented for the CR1 and CR2, respectively.

For the sake of clarity and using the preliminary information obtained from the numerical models, the data associated with the tests in the down- and cross-aisle direction have been treated separately. For the peaks with greater energy content, the associated modal shapes have been reported together with the associated damping (*d*). For the damping evaluation, reference is made to the bandwidth method,[24] which can ensure an accurate estimation of the modal damping coefficient associated to each modal shape highlighted in the frequency domain.

If CR1 is considered, it can be noted that by observing both graphs the bigger quantity of energy is contained in 1.95-Hz frequency, which is associated with a flexural mode shape in transversal direction. This mode involves

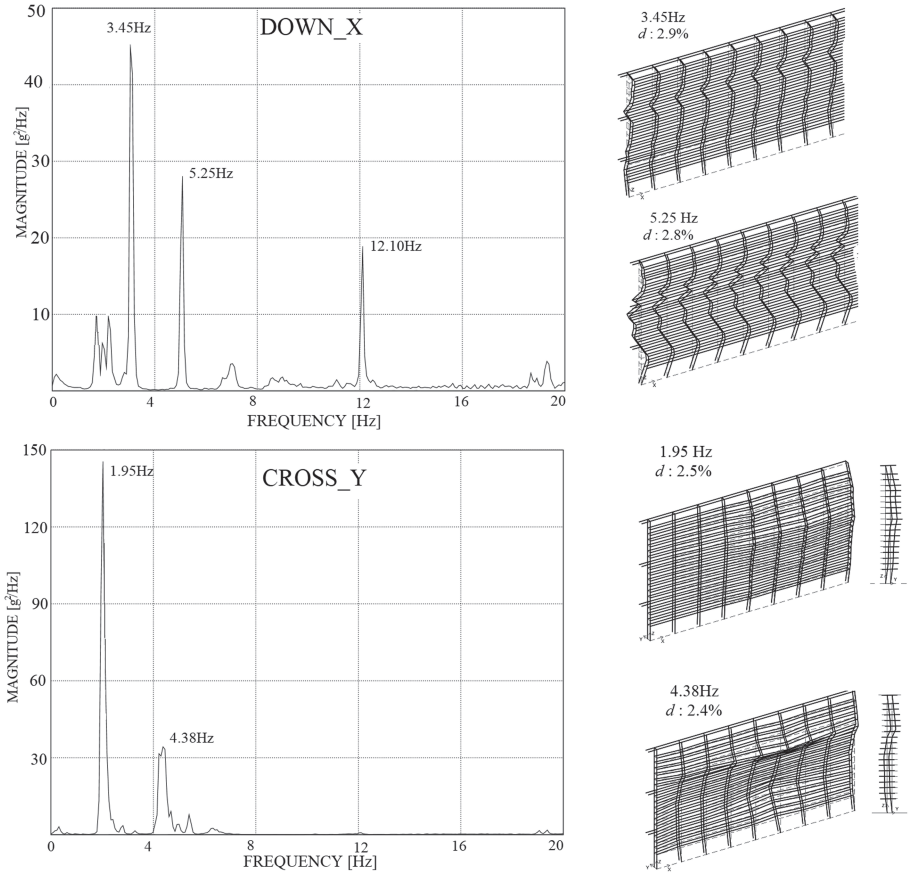

FIGURE 13 Modal identification for CR1 frame: First singular value of the accelerations and deformed shapes associated with predominant peaks

deformations of the points in the same direction with a maximum displacement located at the 11th storage level. The predominant frequency in longitudinal direction is in correspondence of 3.45 Hz and is associated with a flexural mode in longitudinal direction. Further non-negligible energy shows up in the 5.25- and 12.1-Hz range for the longitudinal and 4.38 Hz for the transversal direction. In all the identified modes, the critical damping appears quite low (i.e., significantly lower than 5% that is the default design value allowed in the seismic design of steel structures).

In case of CR2 it can be noted that the highest peaks are in correspondence of 1.15, 2.05 and 5.45 Hz for the down-aisle direction while are in correspondence of 1.88 and 4.22 Hz in the cross-aisle direction. Higher modes can be observed at approximately 8 Hz, in both directions, and in 10.95 Hz in the down-aisle direction. The first predominant frequency is associated with a longitudinal shape that involves all the columns deforming in the same direction. The second one has the same behaviour, but the deformation takes place in the cross-aisle direction. Higher modes are characterised by the inversion of the deformation at a certain height of the CR2. Also, in this case the critical damping (d) appears quite low, always lower than 5%.

As a summary of the detected modes Table 6 can be considered, where the frequency and the damping (d) associated with the first five modes are reported together with the predominant direction of the mode shape. By observing the numerical response, only the first four modes are of interest to characterise the overall racks behaviour, that is, the sum of the modal mass involved reach the 85% of the total mass in both directions.

4.3 | Comparison between modal results and numerical models

Once the modal identification phase is completed, the mode shapes resulting from the application of FDD could be compared with the numerical ones obtained via FE models by using the well-known Modal Assurance Criterion

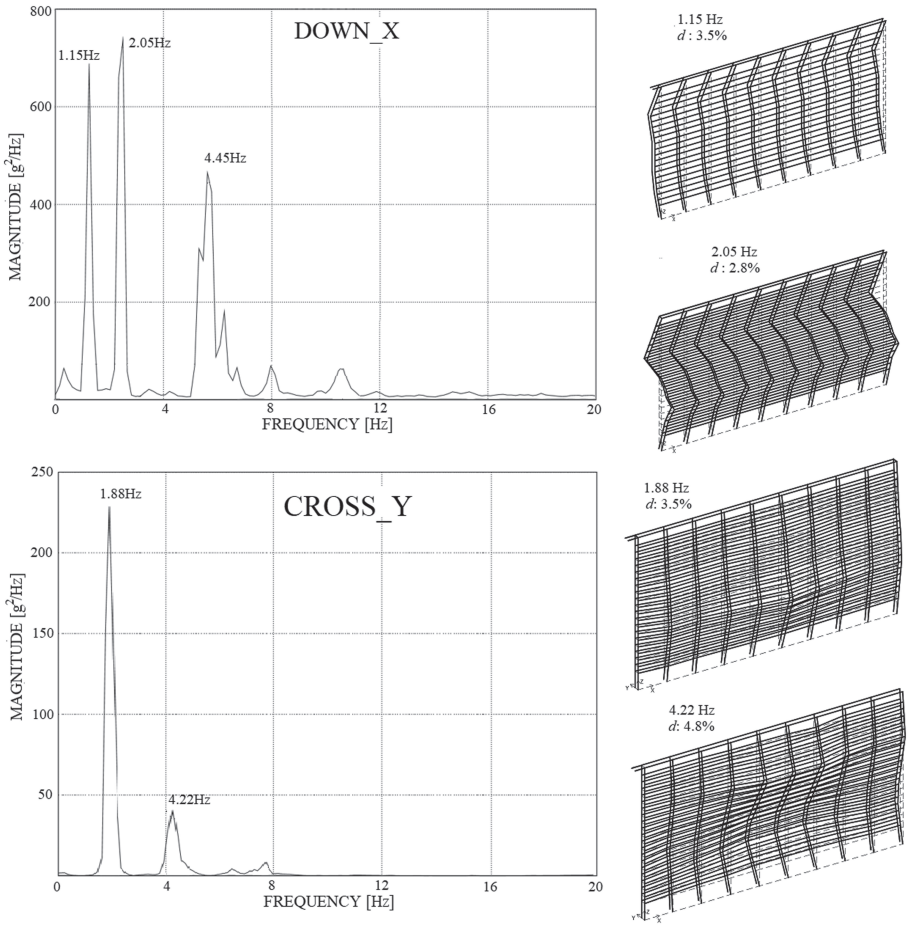

FIGURE 14 Modal identification for CR2 frame: First singular value of the accelerations and deformed shapes associated with predominant peaks

TABLE 6 Summary of the detected modes

	CR1		CR2	
	Frequency	**d**	**Frequency**	**d**
I mode	1.95 Hz (cross)	2.5%	1.15 Hz (down)	3.5%
II mode	3.45 Hz (down)	2.9%	1.88 Hz (cross)	3.5%
III mode	4.38 Hz (cross)	2.4%	2.05 Hz (down)	2.8%
IV mode	5.25 Hz (down)	2.8%	4.22 Hz (cross)	4.8%
V mode	12.1 Hz (down)	2.6%	4.45 Hz (down)	4.9%

(MAC).[25,26] The MAC index is associated with the most commonly used procedure to correlate two sets of mode shape vectors and is defined as follows:

$$MAC(\emptyset_{A,k}, \emptyset_{B,k}) = \frac{\left(\emptyset_{A,k}^T \emptyset_{B,k}\right)^2}{\left(\emptyset_{A,k}^T \emptyset_{A,k}\right)\left(\emptyset_{B,k}^T \emptyset_{B,k}\right)} \tag{4}$$

where $\emptyset_{A,k}$ is related to the data set A (experimental) and $\emptyset_{B,k}$ the related to the data set B (numerical). The MAC index is a coefficient analogous to the correlation coefficient in statistics and ranges from 0 to 1; a value of 1 implies perfect

TABLE 7 MAC and D_F values of CR1

	CR1_A		CR1_B		CR1_C		CR1_D		CR1_E	
Predominant direction	**MAC**	D_F	**MAC**	D_F	**MAC**	D_F	**MAC**	D_F	**MAC**	D_F
cross	0.115	63%	0.008	62%	0.905	12%	0.921	3%	0.951	2%
down	0.015	45%	0.155	43%	0.911	2%	0.665	34%	0.922	8%
cross	0.312	55%	0.588	28%	0.885	6%	0.661	33%	0.841	6%
down	0.502	31%	0.522	29%	0.955	11%	0.811	19%	0.874	23%

TABLE 8 MAC and D_F values of CR2

	CR2_A		CR2_B		CR2_C		CR2_D		CR2_E	
Predominant direction	**MAC**	D_F	**MAC**	D_F	**MAC**	D_F	**MAC**	D_F	**MAC**	D_F
down	0.551	59%	0.815	15%	0.915	6%	0.791	31%	0.651	31%
cross	0.651	24%	0.888	13%	0.815	13%	0.698	29%	0.715	17%
down	0.551	18%	0.841	15%	0.885	10%	0.655	24%	0.825	20%
cross	0.654	58%	0.711	55%	0.665	44%	0.666	39%	0.855	16%

correlation of the two mode shape vectors while a value close to 0 indicates uncorrelated (orthogonal) vectors. In general, a MAC value greater than 0.80 is considered a good match while a MAC value less than 0.40 is considered a poor match. The result is a MAC matrix associated with the comparison between the experimental and numerical eigenvectors.

Moreover, to compare the differences in term of frequencies, parameter D_F has been introduced[27] as

$$D_F = \left| \frac{f_{FEM} - f_{exp}}{f_{FEM}} \right| \cdot 100\,[\%] \tag{5}$$

where f_{FEM} is the frequency value obtained from finite element model and f_{exp} is the one experimentally observed. The lower is D_F and the better is the agreement between the compared frequencies.

Both the principal diagonal of the MAC matrix and D_F have been evaluated for each model proposed in Section 3 and the results are plotted in Tables 7 and 8. As previously discussed, the modal mass in both longitudinal and transversal direction is mainly involved in the first modes; therefore, only four modes have been considered.

Considering CR1, it can be noted that the case _A and _C give the lowest MAC values and the highest D_F coefficients, denoting a bad agreement between the modelling hypothesis and the real structural behaviour. Otherwise, other models give a quite good values of the MAC and D_F index: the best match is represented by the _C model, which is the most rigid one, where the MAC index is always greater than 0.8 and the D_F is lower than 15%.

Also, for CR2 best match is given by the _C model where for the first three modes the MAC results higher than 0.8 and D_F lower than 15%. All the other models give a quite bad value of both indices. In particular, the match with the fourth mode is addressed only considering the _E model, where the MAC results higher than 0.85 with a quite good D_F value.

5 | PRELIMINARY CONCLUSIONS

Old cheese racks require an accurate evaluation of their effective safety with reference to the seismic design approaches currently recommended by provisions. These unconventional structures are characterised by the presence of quite expensive goods (cheese wheels), which must be preserved in case of seismic events. Upon recalling the 2012 seismic event, the collapse of cheese racks led to relevant economic losses for the whole Italian industry sector.

Since the peculiarities of the structural system, which is an unconventional wood-steel composite frame, the behaviour is remarkably influenced mainly by three generally unknown parameters: (i) the degree of stiffness offered by the wood boards; (ii) the degree of restraint offered by the bases and (iii) the stiffness of the connections with the surrounded building. The elastic behaviour of these three parameters can be identified only experimentally and this paper's focus is the description of in situ modal identification tests necessary to this purpose. In particular, the experimental campaign executed on two typical old cheese racks have been considered and described in detail. As demonstrated by the numerical FE analyses, test data are of paramount importance to calibrate the three key parameters, which govern the overall response. It has been demonstrated that also the knowledge of the structural parameters is essential for the precise evaluation of the safety of the cheese racks in both seismic and static design. The assumption of simplified hypothesis for them, showed that the predicted behaviour is quite far from the effective one, as demonstrated by MAC and D_F parameters presented in Tables 6 and 7. When the results associated with the different numerical models were compared to each other it can be noted that, also the critical load multiplier showed a great variation, up to 6 times, thus producing a great dispersion also in the maximum SI (up to 2.6 times different).

The results presented in the paper underline the inadequacy of the traditional and too simplified design assumptions, stressing out the need of a refined calibration of the aforementioned unknown parameters before the design phase of these steel frames. In fact, only after an adequate calibration of the numerical models (optimisation procedure) it is possible to define the more reliable strategy to strengthen these frames against earthquakes. This activity will be carried out from the research team in the near future, according to the well-established procedures already available in literature.[28,29]

ACKNOWLEDGEMENTS

Open Access Funding provided by Politecnico di Milano within the CRUI-CARE Agreement.

AUTHOR CONTRIBUTIONS

Claudio Bernuzzi: Experimental analysis, Conceptualization, Methodology. **Carlo Rottenbacher**: Experimental analysis, Validation, Methodology. **Marco Simoncelli**: Experimental analysis, Data and study validation, Software. **Paolo Venini**: Investigation, Software, methodology. All authors have contributed in the writing-review-editing process of the whole paper.

DATA AVAILABILITY STATEMENT

All the data supporting the findings of this study are available from the corresponding author upon a specific request.

ORCID

Marco Simoncelli https://orcid.org/0000-0002-0542-246X
Paolo Venini https://orcid.org/0000-0002-0023-1197

REFERENCES

1. Braga F, Gigliotti R, Monti G, et al. Speedup of post-earthquake community recovery: the case of precast industrial buildings after the email 2012 earthquake. *Bull Earthq Eng*. 2014;12(5):2405-2418. doi:10.1007/s10518-014-9583-3
2. Bernuzzi C, Simoncelli M. Seismic design of grana cheese cold-formed steel racks. *Buildings*. 2020;10(12):246. doi:10.3390/buildings10120246
3. Tilburgs K. Those peculiar structures in cold-formed steel: "racking & shelving". *Steel Constr*. 2013;6(2):95-106. doi:10.1002/stco.201310016
4. Bernuzzi C, Simoncelli M. EU and US design approaches for steel storage pallet racks with mono-symmetric cross-section uprights. *Thin-Walled Struct*. 2017;113:181-204. doi:10.1016/j.tws.2017.01.014
5. Gabbianelli G, Cavalieri F, Nascimbene R. Seismic vulnerability assessment of steel storage pallet racks. *Ingegneria Sismica*. 2020;37(2):18-40.
6. Gusella F, Orlando M, Spinelli P. Pinching in steel rack joints: numerical modelling and effects on structural response. *Int J Steel Struct*. 2019;19(1):131-146. doi:10.1007/s13296-018-0095-x
7. Bernuzzi C, Gobetti A, Gabbianelli G, Simoncelli M. Unbraced pallet rack design in accordance with European practice-part 1: selection of the method of analysis. *Thin-Walled Struct*. 2015;86:185-207. doi:10.1016/j.tws.2014.06.015
8. Liu SW, Pekoz T, Gao WL, Ziemian RD, Crews J. Frame analysis and design of industrial rack structures with perforated cold-formed steel columns. *Thin-Walled Struct*. 2021;163:107755. doi:10.1016/j.tws.2021.107755

9. Franco A, Massimiani S, Royer-Carfagni G. Passive control of steel storage racks for Parmgiano Reggiano cheese under seismic accelerations. *J Earthq Eng*. 2015;19(8):1222-1259. doi:10.1080/13632469.2015.1049386
10. Filiatrault A, Higgins PS, Wanitkorkul A. Experimental stiffness and seismic response of pallet-type steel storage rack connectors. *Pract Period Struct des Construct*. 2006;11(3):161-170. doi:10.1061/(ASCE)1084-0680(2006)11:3(161)
11. Castiglioni CA, Drei A, Kanyilmaz A. Continuous monitoring of service conditions of a steel storage racking system. *J Earthq Eng*. 2020;3(3):485-505. doi:10.1080/13632469.2018.1453402
12. Simoncelli M, Tagliafierro B, Montuori R. Recent development on the seismic devices for steel storage structures. *Thin-Walled Struct*. 2020;155:106827. doi:10.1016/j.tws.2020.106827
13. Castiglioni CA, Drei A, Kanyilmaz A, Mouzakis HP. Earthquake-induced pallet sliding in industrial racking systems. *J Buildi Eng*. 2018;19:122-133. doi:10.1016/j.jobe.2018.05.004
14. Petrone F, Higgins P, Bissonnette N, Kanvinde A. The cross-aisle seismic performance of storage rack base connections. *J Constr Steel Res*. 2016;122:520-531. doi:10.1016/j.jcsr.2016.04.014
15. EN16681. *Steel static storage systems – adjustable pallet racking systems – principles for seismic design*. Brussels: European commitee for standadization; 2016.
16. EN1998-1-1. *Design of structures for earthquake resistance- part 1: general rules, seismic actions and rules for buildings*. CEN; 2005.
17. Ghahari SF, Abazarsa F, Ebrahimian H, Taciroglu E. Output-only model updating of adjacent buildings from sparse seismic response records and identification of their common excitation. *Struct Control Health Monit*. 2020;27(9):e2597. doi:10.1002/stc.2597
18. Nayek R, Mukhopadhyay S, Narasimhan S. Mass normalized mode shape identification of bridge strctures using a single actuator-sensor pair. *Struct Control Health Monit*. 2018;25(11):e2244. doi:10.1002/stc.2244
19. EN1993-1-1. *Design of steel structures - part 1: general rules and rules for buildings*. CEN; 2005.
20. PCB piezotronics MTS company, www.pcb.com, accessed in 2020.
21. National Instruments, www.ni.com, accessed in 2020.
22. Duhamel P, Vetterli M. Fast Fourier transforms: a review and a state of the art. *Signal Process*. 1990;19(4):259-299. doi:10.1016/0165-1684(90)90158-U
23. Brincker R, Zhang L, Andersen P. Model identification of output only systems using frequency domain decomposition. *Smart Mater Struct*. 2001;10(3):441-445. doi:10.1088/0964-1726/10/3/303
24. Pastor M, Binda M, Harcarik T. Modal Assurance Criterion. *Proc Eng*. 2012;48:543-548. doi:10.1016/j.proeng.2012.09.551
25. Cabboi A, Magalhaes F, Gentile C, Cunha A. Automated modal identification and tracking: application to an iron arch bridge. *Struct Control Health Monit*. 2017;24(1):e1854. doi:10.1002/stc.1854
26. Gentile C, Gallino N. Condition assessment and dynamic system identification of historic suspension footbridge. *Struct Control Health Monit*. 2008;15(3):369-388. doi:10.1002/stc.251
27. Bernuzzi C, Crespi P, Montuori R, et al. Resonance of steel wind turbines: problems and solutions. *Structure*. 2021;32:65-75. doi:10.1016/j.istruc.2021.02.053
28. Dong X, Wang Y. "A comparative study of frequency-domain finite element updating approaches using different optimization procedures." Proceeding of the 8th European Workshop on Structural Health Monitoring (EWSHM), Bilbao, Spain, July 5–8, 2016. 2016.
29. Li D, Dong X, Wang Y. Model updating using sum of squares (SOS) optimization to minimize modal dynamic residuals. *Struct Control Health Monit*. 2018;25:e2263. doi:10.1002/stc.2263

How to cite this article: Bernuzzi C, Rottenbacher C, Simoncelli M, Venini P. Modal identification of storage racks for cheese wheels. *Struct Control Health Monit*. 2022;29(10):e3052. doi:10.1002/stc.3052